Halogen−hydride interaction between Z−X (Z = CN, NC; X = F, Cl, Br) and H−Mg−Y (Y = H, F, Cl, Br, CH3)

ARTICLE *in* THE JOURNAL OF PHYSICAL CHEMISTRY A · APRIL 2011

Impact Factor: 2.69 · DOI: 10.1021/jp200689b · Source: PubMed

3 AUTHORS, INCLUDING:

Afshan Mohajeri
Shiraz University
68 PUBLICATIONS **554** CITATIONS

SEE PROFILE

Mojtaba Nodehi
Ferdowsi University Of Mashhad
31 PUBLICATIONS **170** CITATIONS

SEE PROFILE

THE JOURNAL OF PHYSICAL CHEMISTRY A

ARTICLE

pubs.acs.org/JPCA

Halogen−Hydride Interaction between Z−X (Z = CN, NC; X = F, Cl, Br) and H−Mg−Y (Y = H, F, Cl, Br, CH_3)

Afshan Mohajeri,* Mojtaba Alipour, and Mahboubeh Mousaee

Department of Chemistry, College of Sciences, Shiraz University, Shiraz 71454, Iran

Supporting Information

ABSTRACT: Halogen−hydride interactions between Z−X (Z = CN, NC and X = F, Cl, Br) as halogen donor and H−Mg−Y (Y = H, F, Cl, Br, CH_3) as electron donor have been investigated through the use of Becke three-parameter hybrid exchange with Lee−Yang−Parr correlation (B3LYP), second-order Møller−Plesset perturbation theory (MP2), and coupled-cluster single and double excitation (with triple excitations) [CCSD(T)] approaches. Geometry changes during the halogen−hydride interaction are accompanied by a mutual polarization of both partners with some charge transfer occurring from the electron donor subunit. Interaction energies computed at MP2 level vary from −1.23 to −2.99 kJ/mol for Z−F···H−Mg−Y complexes, indicating that the fluorine interactions are relatively very weak but not negligible. Instead, for chlorine- and bromine-containing complexes the interaction energies span from −5.78 to a maximum of −26.42 kJ/mol, which intimate that the interactions are comparable to conventional hydrogen bonding. Moreover, the calculated interaction energy was found to increase in magnitude with increasing positive electrostatic potential on the extension of Z−X bond. Analysis of geometric, vibrational frequency shift and the interaction energies indicates that, depending on the halogen, CN−X···H interactions are about 1.3−2.0 times stronger than NC−X···H interactions in which the halogen bonds to carbon. We also identified a clear dependence of the halogen−hydride bond strength on the electron-donating or -withdrawing effect of the substituent in the H−Mg−Y subunits. Furthermore, the electronic and structural properties of the resulting complexes have been unveiled by means of the atoms in molecules (AIM) and natural bond orbital (NBO) analyses. Finally, several correlative relationships between interaction energies and various properties such as binding distance, frequency shift, molecular electrostatic potential, and intermolecular density at bond critical point have been checked for all studied systems.

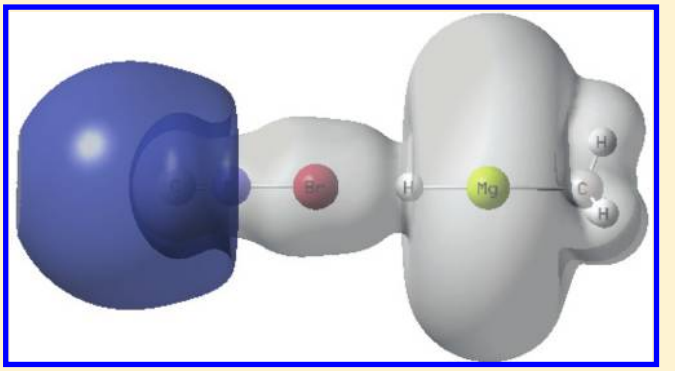

1. INTRODUCTION

Noncovalent interactions play a critical role in chemistry, in particular for intermolecular interaction,[1−3] and supramolecular chemistry[4−7] where the molecular assemblies are usually held together through weak interactions. Among these interactions, the hydrogen bond is probably most frequently and thoroughly investigated.[8−12] Recently, increasing attention has been paid to other intermolecular interactions such as so-called halogen bonds,[13−18] due to their extensive potential utilization in diverse fields such as molecular recognition, drug design, crystal engineering, and versatile materials.[19−28]

A halogen bond is a weak bonding interaction between a polarizable halogen atom X in a molecular species R−X that acts as the Lewis acid and a nucleophilic atomic site Y (such as oxygen, nitrogen, or sulfur) in a neighboring molecular species (Y−R′). The strength of a halogen bond (R−X···Y−R′) varies widely from <0.5 to >40 kcal/mol.[29,30] Halogen bonds share numerous physical properties with the more commonly encountered hydrogen bonds and are often treated analogously to their ubiquitous counterparts.[29,31]

Considering the fact that halogen atoms as well as halogen-bond electron donors (Y) are negatively charged, the existence of halogen bonds is surprising and counterintuitive. However, the formation of halogen bonds can be rationalized in terms of anisotropic distribution of electron density around the halogen atom. Studies of the electrostatic potentials of halogen bonding systems by Auffinger et al.[31] and Politzer and co-workers[32−37] show that X in R−X has a surprising feature: a partial positive electrostatic potential centered on the region of space opposite the R−X bond. This electropositive crown is referred to as the σ-hole, to denote the region of positive charge on the outermost portion of the covalently bonded halogen atom.[38,39] A halogen's σ-hole becomes larger and gains a higher degree of electropositivity as the size of the halogen increases, with a corresponding tendency for the halogen bond to become stronger.

There have been several theoretical[40−50] and experimental studies[51−56] seeking to characterize the geometrical and energetic properties of halogen bonds. With the progress in the study of halogen bonding, some unconventional halogen bonds such as the π-halogen bond,[57] the single-electron halogen bond,[58] and

Received: November 17, 2010
Revised: March 17, 2011
Published: April 01, 2011

Scheme 1

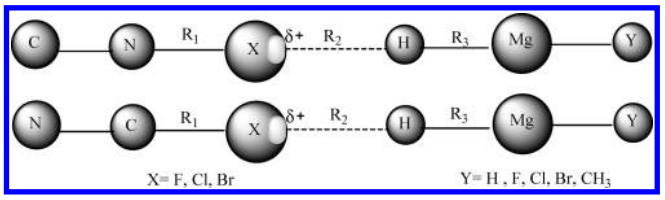

the carbene halogen bond[59] have been proposed. On the basis of the concepts of dihydrogen bonds[60−63] and inverse hydrogen bond,[64] a different type of halogen bonding has been established where a metal hydride acts as the electron donor.[65−67] In such halogen−hydride interactions, the halogen atom acts as a Lewis acid center and the H-atom, with an excess negative charge, like a Lewis base. However, prediction and characterization of halogen−hydride interactions has been the subject of many recent theoretical studies[68−71] since this type of halogen bond plays a similar role as that of dihydrogen bonds.

In this work, we study halogen−hydride bonding as Z−X···H−Mg−Y formed by interaction between Z−X (Z = CN, NC and X = F, Cl, Br) as the Lewis acid and H−Mg−Y (Y = H, F, Cl, Br, CH_3) as the Lewis base. To elucidate the effect of the chemical environment of halogen on the relative strength of the σ-hole, a comparative study has been performed on the interaction of C-bound halogen (C−X) and N-bound halogen (N−X) with Lewis bases (Scheme 1).

We also consider the substituent effect on halogen−hydride interaction by varying X and Y in the halogen and electron donor species, respectively. The nature and properties of the resultant halogen−hydride bonds have been unveiled in the light of geometrical, energetic, and topological parameters, natural population analysis, shifts in vibrational frequencies, and assessment of molecular electrostatic potential. The most relevant aspect of this theoretical work concerns achievement of valuable information on the strength and nature of halogen−hydride bonding, which would be important in crystal engineering.

2. COMPUTATIONAL METHODS

The wave function and density functional theories (WFT and DFT) calculations have been carried out by means of the Gaussian 03 suite of programs.[72] We utilized the most widely used method in WFT procedures, second-order Møller−Plesset perturbation theory (MP2),[73] which covers the essential portion of the correlation energy. This method has been shown to be effective and accurate in determining the equilibrium structure and binding energy for many hydrogen-bonded and other weakly bonded complexes.[74] However, to study the higher-order correlation effect, single-point calculations were performed at the coupled-cluster single and double excitation (with triple excitations) [CCSD(T)] level. In the DFT framework, among the different functionals now available, we have chosen the Becke three-parameter hybrid exchange with Lee−Yang−Parr correlation (B3LYP) hybrid method,[75,76] which is likely the most frequently used because it yields quite reliable geometries and harmonic vibrational frequencies, so it would be interesting to assess its behavior for the description of halogen−hydride bonds.

The geometries and wave functions of all isolated species and halogen-bonded complexes were fully optimized at MP2 and B3LYP levels without any symmetry constraints. All calculations have been performed with the 6-311++G(d,p) basis set. The stationary structures (monomers and complexes) obtained were characterized as minima by harmonic vibrational frequency calculations (all the frequencies were positive).

Interaction energies were evaluated by using the supermolecule method for the difference between the energy of a complex and the energy sum of the isolated subsystems forming the complex. The basis-set superposition error (BSSE) was eliminated by the standard counterpoise correction method of Boys and Bernardi.[77]

The bonding of the systems under scrutiny was analyzed by means of the atoms in molecules theory (AIM)[78] with the help of the AIM 2000 software.[79] In the framework of the AIM theory, we have evaluated the electron density at different bond critical points (BCP). The existence of a BCP in the region between the halogen atom and the hydrogen of the metal hydride subunit will

Table 1. Halogen−Hydride Distance (R_2) and Percentage Increments in Z−X (ΔR_1) and H−Mg (ΔR_2) Bonds in Halogen-Bonded Complexes with Respect to Isolated Monomers[a]

complex	ΔR_1 (%)	R_2 (Å)	ΔR_2 (%)
NC−F···H−Mg−H	−0.13	2.955	0.05
NC−F···H−Mg−F	−0.07	2.961	0.02
NC−F···H−Mg−Cl	−0.07	2.924	0.06
NC−F···H−Mg−Br	−0.07	2.929	0.03
NC−F···H−Mg−CH_3	−0.14	2.934	−0.01
NC−Cl···H−Mg−H	0.12	2.851	0.13
NC−Cl···H−Mg−F	0.10	2.902	0.07
NC−Cl···H−Mg−Cl	0.10	2.879	0.12
NC−Cl···H−Mg−Br	0.11	2.876	0.08
NC−Cl···H−Mg−CH_3	0.10	2.832	0.06
NC−Br···H−Mg−H	0.36	2.764	0.21
NC−Br···H−Mg−F	0.29	2.825	0.11
NC−Br···H−Mg−Cl	0.30	2.817	0.19
NC−Br···H−Mg−Br	0.27	2.815	0.14
NC−Br···H−Mg−CH_3	0.38	2.740	0.14
CN−F···H−Mg−H	−0.02	2.777	0.04
CN−F···H−Mg−F	0.02	2.793	0.01
CN−F···H−Mg−Cl	0.02	2.759	0.05
CN−F···H−Mg−Br	0.05	2.763	0.02
CN−F···H−Mg−CH_3	−0.04	2.760	0.02
CN−Cl···H−Mg−H	0.72	2.528	0.18
CN−Cl···H−Mg−F	0.52	2.609	0.08
CN−Cl···H−Mg−Cl	0.54	2.592	0.15
CN−Cl···H−Mg−Br	0.56	2.591	0.11
CN−Cl···H−Mg−CH_3	0.80	2.505	0.14
CN−Br···H−Mg−H	3.25	2.127	0.80
CN−Br···H−Mg−F	1.63	2.322	0.30
CN−Br···H−Mg−Cl	1.72	2.302	0.40
CN−Br···H−Mg−Br	1.76	2.299	0.41
CN−Br···H−Mg−CH_3	4.26	2.048	1.01

[a] Calculated at MP2/6-311++G(d,p) level.

permit us not only to establish the existence of a halogen−hydride bond but also to quantitatively estimate its strength. Natural population analysis (NPA) was also employed to describe the state of charge transfer upon complexation by use of the natural bond orbital (NBO)[80] program implemented in Gaussian 03. Moreover, the molecular electrostatic potentials (MEP)[81] of halogen-bound monomers were gained with a view to estimating the electrostatic contribution in halogen−hydride bonding. AIM and NBO analyses and MEP calculations were conducted on the MP2-optimized structures.

3. RESULTS AND DISCUSSION

3.1. Geometrics and Frequency Shifts. The systems studied form stable complexes with $C_{\infty v}$ symmetry for Y = H, F, Cl, and Br and C_{3v} for Y = CH_3. Table 1 presents some of the MP2 geometrical characteristics of the analyzed systems shown in Scheme 1. The X···H intermolecular distances (R_2) as well as the changes of the X(F, Cl, Br)−Z(CN, NC) and H−Mg bond lengths as a result of complexation are reported. These changes (ΔR) are calculated as the increments of Z−X and H−Mg bond lengths relative to the bonds not involved in the interaction. In other words, ΔR (%) = $(R - R_0)/R_0 \times 100$, where R is the corresponding bond length in the complex and R_0 corresponds to the reference bond not involved in the interaction and obtained through full geometry optimization of the monomeric system. As can be seen from Table 1, the intermolecular X···H distances varies between 2.740 and 2.961 Å for NC−X···H−Mg−Y complexes, while it is reduced to 2.048−2.793 Å in CN−X···H−Mg−Y systems. The calculated binding distances are equal to or less than the sum of the van der Waals (vdW) radii of the halogen and hydrogen atoms (vdW radii for H, F, Cl, and Br are 1.2, 1.47, 1.175, and 1.85 Å, respectively),[82] indicating attractive force between the two subunits. The only exception is fluorine complexes in which F···H distances are somewhat longer than the sum of vdW radii of fluorine and hydrogen atoms, implying a particularly weak interaction in these complexes.

The results show that the intermolecular distances are contracted by about 0.05−0.1 Å when the fluorine atom in Z−F···H−Mg−Y is replaced by chlorine, and a bigger contraction is observed when chlorine atom is replaced by bromine. If we assume that the X···H distance roughly corresponds to the strength of the interaction, then Br complexes with smaller distances are more stable than the Cl and F counterparts.

It is known that evidence of H-bond formation, for such typical interactions as O−H···O or N−H···O, is connected with elongation of the proton-donating bond. For the systems considered here, there are elongations of the Z−X and H−Mg bonds for most complexes. The exceptions are fluorine-containing complexes, in which Z−F bond lengths shortened during complex formation in some cases. The computed increments in Z−X bond lengths, ΔR_1, reveal that the maximum elongations occurred in Z−Br bonds. As the intermolecular X···H distance decreases, the halogen donor Z−X distance increases. The increments in Z−X bonds are mostly less than 1% with a few exceptions in CN−Br-containing complexes, in which the increments enhance up to about 4.3%. Moreover the increments in H−Mg bonds, ΔR_2, are almost all less than 1%, indicating that the structures of H−Mg−Y fragments remain unchanged as a result of complexation.

During complex formation, the bond length variation has strong effects on the frequencies of Z−X and H−Mg bonds in comparison with the noninteracting species. Along with elongation of the Z−X bond length, vibrational frequency of this bond suffers a substantial reduction upon formation of the X···H bond. The amounts of calculated red shifts are reported in Table 2 for all 30 studied complexes. In each series the red shifts of Z−Br bonds are remarkably greater than those obtained for Z−Cl bonds. The largest shifts in Z−X frequency occur in CN−Br complexes, while the smallest shifts are observed in NC−F-containing systems. Among all studied complexes, the C−X frequency in NC−X-containing complexes has a red shift less than 40.50 cm^{-1}, while the shift in N−X frequency in CN−X complexes climbs to nearly 192.40 cm^{-1}, indicating a better halogen donor.

On the other hand, the H−Mg vibration exhibits a blue shift although H−Mg bonds are lengthened upon complexation. The shift in the H−Mg frequency depends on the nature of the

Table 2. Change in Vibrational Frequencies of Z−X and H−Mg Bonds[a] and Molecular Electrostatic Potentials[b]

complex	$\Delta\nu_{Z-X}$ (cm^{-1})	$\Delta\nu_{H-Mg}$ (cm^{-1})	MEP (kJ/mol)
NC−F···H−Mg−H	3.13	4.20	56.41
NC−F···H−Mg−F	0.79	2.71	56.25
NC−F···H−Mg−Cl	0.54	2.86	56.25
NC−F···H−Mg−Br	0.78	2.78	56.25
NC−F···H−Mg−CH_3	2.42	6.28	56.45
NC−Cl···H−Mg−H	−17.84	12.46	197.47
NC−Cl···H−Mg−F	−11.24	8.32	197.46
NC−Cl···H−Mg−Cl	−12.02	8.30	197.46
NC−Cl···H−Mg−Br	−12.24	8.87	197.46
NC−Cl···H−Mg−CH_3	−19.03	17.52	197.47
NC−Br···H−Mg−H	−31.35	15.20	235.04
NC−Br···H−Mg−F	−19.63	14.54	234.93
NC−Br···H−Mg−Cl	−19.94	11.16	234.94
NC−Br···H−Mg−Br	−21.26	10.98	234.90
NC−Br···H−Mg−CH_3	−40.41	10.86	235.06
CN−F···H−Mg−H	−8.70	4.06	50.39
CN−F···H−Mg−F	−5.59	2.31	50.35
CN−F···H−Mg−Cl	−7.04	3.11	50.35
CN−F···H−Mg−Br	−6.43	2.48	50.35
CN−F···H−Mg−CH_3	−9.02	7.16	50.39
CN−Cl···H−Mg−H	−107.11	15.37	211.05
CN−Cl···H−Mg−F	−57.91	8.80	215.11
CN−Cl···H−Mg−Cl	−61.40	6.37	210.56
CN−Cl···H−Mg−Br	−61.54	7.07	210.60
CN−Cl···H−Mg−CH_3	−123.41	3.37	211.27
CN−Br···H−Mg−H	−167.47	7.01	266.77
CN−Br···H−Mg−F	−106.60	8.78	261.45
CN−Br···H−Mg−Cl	−115.00	2.63	261.74
CN−Br···H−Mg−Br	−105.77	1.86	261.87
CN−Br···H−Mg−CH_3	−192.37	31.32	270.06

[a] Calculated at B3LYP/6-311++G(d,p) level. [b] MEP was calculated at a point on the outer side of halogen, along the extension of the respective covalent bond, at which the electron density corresponds to 0.001 au (electrons/$bohr^3$) at MP2/6-311++G(d,p) level.

dx.doi.org/10.1021/jp200689b |J. Phys. Chem. A 2011, 115, 4457–4466

Table 3. Interaction Energies and Counterpoise-Corrected Interaction Energies Calculated at Different Levels

complex	ΔE(B3LYP) (kJ/mol)	ΔE_{corr}(B3LYP) (kJ/mol)	ΔE(MP2) (kJ/mol)	ΔE_{corr}(MP2) (kJ/mol)	ΔE[CCSD(T)] (kJ/mol)
NC−F···H−Mg−H	−2.30	−1.74	−3.29	−2.21	−3.31
NC−F···H−Mg−F	−1.11	−0.57	−2.45	−1.38	−2.48
NC−F···H−Mg−Cl	−1.48	−0.51	−2.92	−1.23	−3.01
NC−F···H−Mg−Br	−1.11	−0.59	−2.58	−1.41	−2.67
NC−F···H−Mg−CH_3	−2.64	−2.04	−3.75	−2.56	−3.76
NC−Cl···H−Mg−H	−9.05	−7.86	−10.21	−8.37	−10.03
NC−Cl···H−Mg−F	−5.50	−4.37	−7.74	−5.80	−7.49
NC−Cl···H−Mg−Cl	−6.02	−4.31	−8.26	−5.78	−8.08
NC−Cl···H−Mg−Br	−5.69	−4.48	−7.95	−5.83	−7.81
NC−Cl···H−Mg−CH_3	−10.16	−8.77	−11.24	−9.03	−10.97
NC−Br···H−Mg−H	−14.50	−13.45	−13.85	−12.28	−13.34
NC−Br···H−Mg−F	−8.86	−7.85	−10.30	−8.62	−9.73
NC−Br···H−Mg−Cl	−9.43	−7.85	−10.81	−8.70	−10.33
NC−Br···H−Mg−Br	−9.05	−8.10	−10.44	−8.77	−9.97
NC−Br···H−Mg−CH_3	−16.04	−15.00	−15.12	−13.34	−14.49
CN−F···H−Mg−H	−2.64	−1.80	−4.21	−2.82	−3.94
CN−F···H−Mg−F	−1.51	−0.78	−3.25	−1.81	−3.17
CN−F···H−Mg−Cl	−1.90	−0.64	−3.74	−1.63	−3.71
CN−F···H−Mg−Br	−1.54	−0.73	−3.43	−1.67	−3.42
CN−F···H−Mg−CH_3	−2.98	−2.09	−4.72	−2.99	−4.40
CN−Cl···H−Mg−H	−17.46	−15.62	−15.63	−13.02	−14.23
CN−Cl···H−Mg−F	−10.71	−9.10	−11.62	−9.09	−8.85
CN−Cl···H−Mg−Cl	−11.54	−9.16	−12.37	−9.15	−11.39
CN−Cl···H−Mg−Br	−11.26	−9.45	−12.02	−9.22	−11.09
CN−Cl···H−Mg−CH_3	−19.52	−17.55	−17.09	−14.15	−15.50
CN−Br···H−Mg−H	−35.63	−33.67	−27.34	−23.82	−22.37
CN−Br···H−Mg−F	−21.75	−19.95	−19.06	−16.05	−17.28
CN−Br···H−Mg−Cl	−22.76	−20.26	−19.84	−16.26	−16.54
CN−Br···H−Mg−Br	−22.76	−20.96	−19.50	−16.43	−16.23
CN−Br···H−Mg−CH_3	−40.32	−38.22	−30.77	−26.42	−24.72

halogen donor molecule. The greater blue shift has been observed in the bromine-containing molecules with a maximum of 31.32 cm^{-1} in CN−Br···H−Mg−CH_3 complex. The computed values of $\Delta\nu$ in Table 2 demonstrate that the blue shift of H−Mg stretch is less than the red shift of Z−X stretch. Moreover, the shifts in H−Mg stretching frequencies are not as systematic as those observed for the shifts in Z−X frequencies.

3.2. Interaction Energy. The discussed trends within the geometrical details find confirmation in the energetics compiled in Table 3. As can be seen at first glance, the interaction energy trends in each series are very similar for MP2 and B3LYP methods. However, there exist some inconsistencies when we compare ΔE_{corr}(B3LYP) and ΔE_{corr}(MP2) values molecule-per-molecule. For instance, in CN−F complexes, the interaction energy is underestimated by B3LYP, while for CN−Br-containing complexes, B3LYP overestimates the interaction energies.

In order to establish whether a high level of electron correlation is required to adequately describe these bonds, we compared the interaction energies computed with MP2 and B3LYP methods with those obtained at the CCSD(T) level. The interaction energies calculated at MP2 level with the counterpoise-corrected geometries differ from those at CCSD(T) level by about 0.2−2.2 kJ/mol, and hence one may rely on the lower level of theory to get reasonably good estimates for the energies of halogen−hydride bonds. As a matter of fact, as shown in Figures S1 and S2 in Supporting Information, the correlation between MP2 and CCSD(T) methods is very good. The correlation between B3LYP and CCSD(T) estimates is slightly poorer but still good, which means that the B3LYP method correctly reproduces the stability trends obtained with the much more expensive CCSD(T) approach. Finally, it should be mentioned that in spite of the differences in energetics obtained by B3LYP and MP2 methods, the bonding picture obtained from these methods is essentially the same.

As deduced from Table 3, the computed values of BSSE at the MP2 level range from 1.07 kJ/mol for the NC−F···H−Mg−F

dx.doi.org/10.1021/jp200689b |J. Phys. Chem. A 2011, 115, 4457–4466

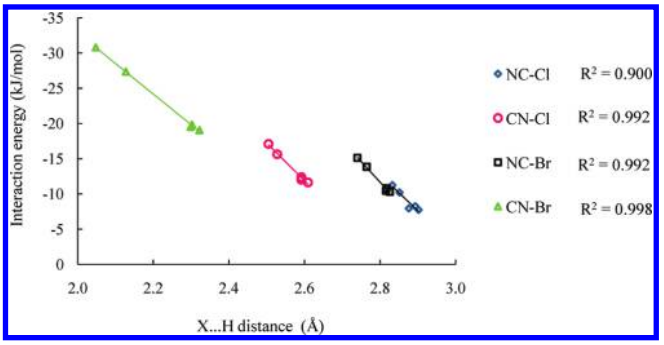

Figure 1. Relationship of interaction energy and binding distance, as well as linear correlation coefficients for each family of studied compounds calculated at MP2/6-311++G(d,p) level.

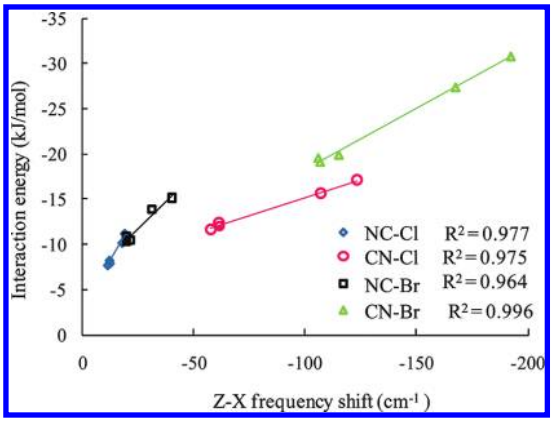

Figure 2. Relationship of interaction energy and Z−X frequency shift, as well as linear correlation coefficients for each family of studied compounds calculated at MP2/6-311++G(d,p) level.

complex to 4.35 kJ/mol for the CN−Br···H−Mg−CH_3 complex. The percentage of BSSE relative to the raw interaction energy is in a range of 11−56% for CN−X- and NC−X-complexes, indicating the significance of BSSE in these systems.

After correction for BSSE, the interaction energies for NC−X···H−Mg−Y and CN−X···H−Mg−Y complexes, respectively, span a range from −1.23 to −13.34 kJ/mol and from −1.63 to −26.42 kJ/mol at the MP2 level, indicating that the CN−X subunit acts as a stronger Lewis acid than NC−X. When CN−X and NC−X complexes are compared, the interaction energies are about 1.3−2.0 times larger when the halogen is bound to nitrogen. Moreover, when halogen donors having the same Z group are compared, it is apparent that the strength of interactions decreases in the order Br > Cl > F.

As a result of a combination of extreme electronegativity and limited polarizability, the fluorine atom is frequently deemed to not participate in halogen-bonding interactions. The electron density distribution around F is nearly spherical rather than anisotropic, and consequently, F always acts as hydrogen-bond acceptor. Nevertheless, several recent theoretical studies have apparently shown that the fluorine atom does have the capability of forming halogen bonds if it is bound to a very strong electron-withdrawing group.[83,84] Here, we showed that the F···H interaction occurs at a larger distance and the interaction energies are less than 3 kJ/mol. The calculated interaction energies for NC−F···H−Mg−Y complexes are, respectively, about 25% and 16% of those obtained for their chlorine and bromine counterparts. For the stronger CN−X···H−Mg−Y complexes, the CN−F interactions are about 20% and 12% of those obtained for CN−Cl and CN−Br complexes. Moreover, the results show that the strength of fluorine−hydride interaction is less affected by the electron-withdrawing power of the Z group attached to F, and the interaction energies span almost the same order for all fluorine-containing complexes.

Figure 1 shows the dependence between X···H distance and interaction energy. Due to low energy of fluorine complexes and better arrangement of our figures, we exclude fluorine-containing systems from this figure and other correlation diagrams in forthcoming sections. For all studied systems, one can observe the monotonic enhancement of the interaction energy with a decrease of the X···H distance. Linear relationships with different slopes have been observed in each series when the halogen and Z group are constant but Y varies. Regression coefficients of linear fits are also reported for each series.

Such a relationship is also observed between interaction energy and amount of red shift in Z−X frequency. Generally, in each series Z−X···H−Mg, the stronger the halogen−hydride interaction, the larger the red shift of Z−X stretch becomes; as illustrated by the linear correlations between interaction energy and Z−X red shift in Figure 2. In comparison to the red shift in Z−X frequency, the blue shifts of H−Mg stretch have less perfect correlation with interaction energies.

3.3. Electrostatic Potential. The molecular electrostatic potential (MEP) at a given point in the vicinity of a molecule is the force acting on a positive test charge located at this point through the electrical charge cloud generated from electrons and nuclei of the molecule. The MEP that the electrons and nuclei of a molecule create in the surrounding space is given by the following equation:[81]

$$V(\mathbf{r}) = \sum_{\alpha} \frac{Z_\alpha}{|\mathbf{R}_\alpha - \mathbf{r}|} - \int \frac{\rho(\mathbf{r}')}{|\mathbf{r}' - \mathbf{r}|}\, d\mathbf{r}' \qquad (1)$$

in which Z_α is the charge on nucleus α, located at $\mathbf{R}_\alpha$, and $\rho(\mathbf{r})$ is the electronic density. The first term in the above equation refers to the bare nuclear potential and the second to the electronic contribution. The MEP can also be interpreted from the classical electrostatics point of view; the molecule provides a potential around itself that is seen by a point like positive probe charge, approaching or avoiding regions where the MEP is negative or positive, respectively. Despite the fact that the molecular charge distribution remains unperturbed through the external test charge (no polarization occurs), the electrostatic potential of a molecule is still a good guide in assessing the molecule's reactivity toward positively or negatively charged reactants. $V(\mathbf{r})$ is a real property of a system, a physical observable, which can be determined experimentally by diffraction techniques[85] and computationally. Its sign in any region depends upon whether the positive contributions of the nuclei or the negative ones of the electrons are dominant there. This quantity has been widely used in many different areas[86−90] including electronic molecular structure, reactivity, and intermolecular forces.[91] Moreover, electrostatic potential is an effective means of analyzing and predicting noncovalent interactions.[92−94] For example, a variety of condensed-phase physical properties that depend upon noncovalent interactions can be expressed analytically in terms of $V(\mathbf{r})$; this includes heats of phase transitions, solubilities and solvation energies, partition coefficients, boiling points and critical constants, viscosities, diffusion coefficients, surface tensions, etc.[95]

dx.doi.org/10.1021/jp200689b |J. Phys. Chem. A 2011, 115, 4457–4466

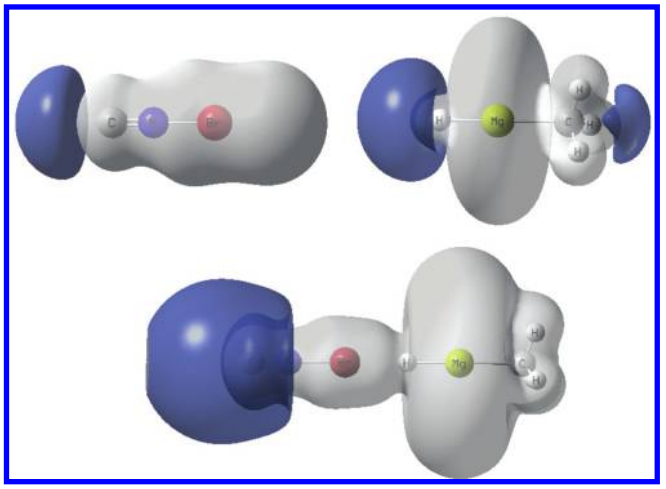

Figure 3. Electrostatic potential isosurfaces (0.025 au) of CN−Br and H−Mg−CH_3 subunits as well as their complex CN−Br···H−Mg−CH_3, calculated at the MP2/6-311++G(d,p) level. Blue and gray colors represent the negative and positive molecular electrostatic potentials, respectively.

To have a clear understanding of the role of MEP in the halogen−hydride interaction, we plotted the electrostatic potential maps of CN−Br and H−Mg−CH_3 as well as their complex CN−Br···H−Mg−CH_3 as illustrative examples in Figure 3. Clearly, a negative electrostatic potential (blue color) is present at the H end of the H−Mg−CH_3 subunit, whereas a positive one (gray color) is observed at the Br end along the extension of the CN−Br bond. Also, a shift in negative electrostatic potential toward the CN group of the halogen donor molecule is seen upon complexation. To gain a deeper insight into the electrostatic contribution of halogen−hydride bonding, we have calculated the MEP values for the monomers Z−X (Table 2). Considering the excellent linearity of the Z−X···H−Mg contacts in the halogen−hydride-bonded complexes, the MEPs at a point on the outer side of halogen along the extension of the respective covalent bond at which the electron density corresponds to 0.001 au (electrons/bohr^3) are taken into account. The 0.001 au contour has been demonstrated to lie beyond atomic van der Waals radii (except for that of hydrogen);[96] thus the electrostatic potential on this surface represents what an approaching entity sees before interaction.

The calculated MEP values at a point on the extension of Z−X covalent bond at which the electron density corresponds to 0.001 au (electrons/bohr^3) are collected in the last column of Table 2. It can be readily appreciated that the MEP values are notably greater in chlorine- and bromine-containing complexes than the corresponding MEP values for fluorine complexes. In addition, due to larger polarizability of Br with respect to Cl, the positive electrostatic potential on the extension of the Z−X bond is also larger for bromine. A close look at the relationship between interaction energies and calculated MEPs shows that there is a linear correlation, as displayed in Figure 4. It thus supports the general understanding that the strength of halogen bond correlates with the positive electrostatic potential on the extension of the covalent bond to the halogen. In view of resultant regression coefficients, it could be concluded that the molecular electrostatic potential is, in general, a good descriptor in prediction of the halogen−hydride interaction energy. Among all studied

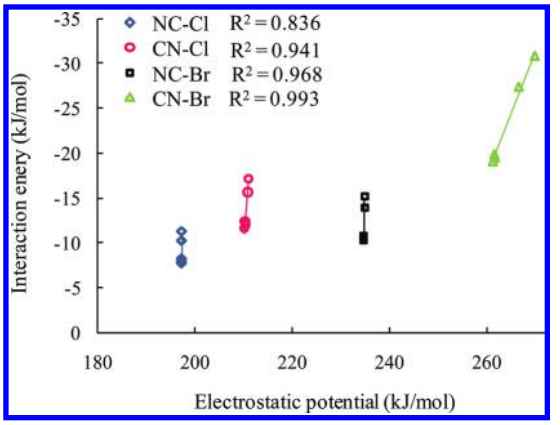

Figure 4. Relationship of interaction energy and electrostatic potential as well as linear correlation coefficients for each family of studied compounds, calculated at MP2/6-311++G(d,p) level.

systems, better correlativities were found for the bromine-containing complexes.

3.4. AIM and NBO Analyses. A topological analysis of the electron density of the system under investigation shows the existence of bond critical points (BCP) associated with the halogen−hydride bond. The properties at the BCPs were first analyzed in terms of the electron density (ρ). Then we provided more specific information concerning the nature of interaction through the Laplacian and energetic properties of BCP. The electron density at BCP of Z−X, H−Mg, and X···H bonds is reported in Table 4. It can be observed that the electron density corresponding to X···H is typical of the interactions between closed-shell systems and lies within the conventional range of closed-shell interactions such as hydrogen bond (0.002−0.04 au).[97] The electron densities are, respectively, within the range of 0.0029−0.0101 and 0.0040−0.0403 for NC−X···H−Mg−Y and CN−X···H−Mg−Y complexes. Moreover, analysis of the results in Table 4 shows that, along with the enhancement of electron density at X···H in the stronger interactions, there exists a reduction in the electron density at Z−X BCPs in these complexes. This observation is in line with the Z−X bond elongation, which has been discussed before. On the contrary to definite variation of electron density at Z−X bond, the electron density changes at H−Mg bonds are insensible and the electron densities remain almost in the same order in all complexes.

For hydrogen bonds, there may be a relationship between the interaction energy and topological parameters at the BCP.[98] Here, the existence of such a relationship has been checked for the halogen−hydride interaction. Figure 5 presents the linear correlation between interaction energies and $\rho_{X\cdots H}$ at the intermolecular BCPs in chlorine and bromine complexes. Although all regression coefficients are greater than 0.96, better correlativities were found for bromine complexes.

The interactions can be further characterized by evaluating the Laplacian of electron density, $\nabla^2\rho(r_c)$, associated with the X···H contact:

$$\left(\frac{\hbar^2}{4m}\right)\nabla^2\rho(r_c) = 2G(r_c) + V(r_c) \qquad (2)$$

where $G(r_c)$is the kinetic energy density, which is always positive. $V(r_c)$ is the potential energy density and must be negative.[99] A negative $\nabla^2\rho(r_c)$ shows the excess potential energy at BCP

Table 4. Parameters at the X···H Bond Critical Point as Well as Electron Densities at the BCP of Z−X and H−Mg Bonds[a]

complex	$\rho(r_c)$ (au)	$\nabla^2\rho(r_c)$ (au)	$H(r_c)$ (au)	$G(r_c)$ (au)	$V(r_c)$ (au)	$-G(r_c)/V(r_c)$	ρ_{Z-X} (au)	ρ_{H-Mg} (au)
NC−F···H−Mg−H	0.0030	0.0128	0.0006	0.0026	−0.0020	1.327	0.3151	0.0525
NC−F···H−Mg−F	0.0029	0.0124	0.0006	0.0025	−0.0019	1.341	0.3141	0.0547
NC−F···H−Mg−Cl	0.0031	0.0136	0.0007	0.0027	−0.0021	1.318	0.3141	0.0550
NC−F···H−Mg−Br	0.0031	0.0132	0.0007	0.0027	−0.0020	1.321	0.3141	0.0550
NC−F···H−Mg−CH_3	0.0032	0.0136	0.0006	0.0027	−0.0021	1.310	0.3154	0.0521
NC−Cl···H−Mg−H	0.0069	0.0240	0.0010	0.0050	−0.0040	1.240	0.2523	0.0519
NC−Cl···H−Mg−F	0.0061	0.0216	0.0010	0.0044	−0.0035	1.276	0.2524	0.0542
NC−Cl···H−Mg−Cl	0.0063	0.0224	0.0010	0.0047	−0.0037	1.262	0.2524	0.0545
NC−Cl···H−Mg−Br	0.0064	0.0228	0.0010	0.0047	−0.0037	1.260	0.2523	0.0544
NC−Cl···H−Mg−CH_3	0.0072	0.0248	0.0010	0.0052	−0.0043	1.228	0.2525	0.0516
NC−Br···H−Mg−H	0.0096	0.0288	0.0009	0.0063	−0.0054	1.169	0.1903	0.0514
NC−Br···H−Mg−F	0.0083	0.0256	0.0009	0.0055	−0.0046	1.199	0.1909	0.0539
NC−Br···H−Mg−Cl	0.0084	0.0260	0.0009	0.0056	−0.0047	1.194	0.1909	0.0540
NC−Br···H−Mg−Br	0.0085	0.0260	0.0009	0.0056	−0.0047	1.194	0.1910	0.0540
NC−Br···H−Mg−CH_3	0.0101	0.0300	0.0009	0.0066	−0.0057	1.159	0.1901	0.0511
CN−F···H−Mg−H	0.0043	0.0172	0.0007	0.0037	−0.0030	1.223	0.3840	0.0525
CN−F···H−Mg−F	0.0040	0.0164	0.0007	0.0035	−0.0028	1.237	0.3830	0.0548
CN−F···H−Mg−Cl	0.0043	0.0176	0.0007	0.0037	−0.0030	1.222	0.3831	0.0551
CN−F···H−Mg−Br	0.0042	0.0176	0.0007	0.0037	−0.0030	1.224	0.3827	0.0550
CN−F···H−Mg−CH_3	0.0045	0.0180	0.0007	0.0038	−0.0031	1.213	0.3844	0.0522
CN−Cl···H−Mg−H	0.0125	0.0396	0.0010	0.0090	−0.0080	1.120	0.2306	0.0515
CN−Cl···H−Mg−F	0.0149	0.0476	0.0010	0.0108	−0.0098	1.106	0.2237	0.0540
CN−Cl···H−Mg−Cl	0.0107	0.0352	0.0010	0.0078	−0.0068	1.146	0.2325	0.0542
CN−Cl···H−Mg−Br	0.0107	0.0352	0.0010	0.0078	−0.0068	1.147	0.2324	0.0541
CN−Cl···H−Mg−CH_3	0.0131	0.0412	0.0010	0.0094	−0.0084	1.113	0.2298	0.0511
CN−Br···H−Mg−H	0.0335	0.0788	−0.0017	0.0213	−0.0230	0.928	0.1495	0.0489
CN−Br···H−Mg−F	0.0214	0.0596	0.0007	0.0142	−0.0135	1.054	0.1598	0.0526
CN−Br···H−Mg−Cl	0.0224	0.0616	0.0006	0.0148	−0.0142	1.044	0.1592	0.0527
CN−Br···H−Mg−Br	0.0225	0.0620	0.0006	0.0149	−0.0143	1.042	0.1589	0.0526
CN−Br···H−Mg−CH_3	0.0403	0.0848	−0.0040	0.0252	−0.0291	0.864	0.1436	0.0477

[a] Calculated at MP2/6-311++G(d,p) level. Parameters: $\rho(r_c)$, electron density; $\nabla^2\rho(r_c)$, Laplacian; $H(r_c)$, electron energy density; $G(r_c)$, electron kinetic energy density; $V(r_c)$, electron potential energy density; $-G(r_c)/V(r_c)$, ratio of kinetic to potential electron energy density; and ρ_{Z-X} and ρ_{H-Mg}, electron densities at the BCP of Z−X and H−Mg bonds.

introducing electronic charge concentration in the internuclear region and implies a shared interaction, as in covalent bonds. A positive value for $\nabla^2\rho(r_c)$, in contrast, shows the greater contribution of kinetic energy and the positive curvature of $\rho(r)$ along the interaction line, as the Pauli exclusion principle leads to a relative depletion of charge density in the interatomic surface. Thus the interaction is dominated by the contraction of charge density away from the interatomic surface toward each interaction species (closed-shell interaction). The results in Table 4 reveal that the values of $\nabla^2\rho_{X\cdots H}$ are all positive, with a range of 0.0124−0.0300 and 0.0164−0.0848 au for NC−X···−Mg−Y and CN−X···H−Mg−Y complexes, respectively. These values are within the commonly accepted values of normal hydrogen bonding (0.02−0.15 au).[97]

It has been shown that total electron energy density $H(r_c)$, the sum of kinetic and potential energy densities at BCP, is an even more sensitive index for weak interactions:[100]

$$H(r_c) = G(r_c) + V(r_c) \quad (3)$$

Interactions exhibit a covalent nature when $H(r_c) < 0$ since electrons at BCPs are stabilized in the region, whereas in closed-shell interactions, as in normal H-bonds, $H(r_c) > 0$ due to destabilization of electrons at BCPs. The condition in which $|V(r_c)| < 2G(r_c)$ and $|V(r_c)| > G(r_c)$ provides positive value for $\nabla^2\rho(r_c)$, leading to closed-shell interaction, while $H(r_c)$ is negative and shows shared interaction. This type of interaction is characterized to be partially covalent and partially electrostatic.[98] Moreover, a $G(r_c)/V(r_c)$ ratio greater than 1 generally indicates a noncovalent interaction, and the ratio becomes smaller than unity as the covalent nature increases.

dx.doi.org/10.1021/jp200689b |J. Phys. Chem. A 2011, 115, 4457–4466

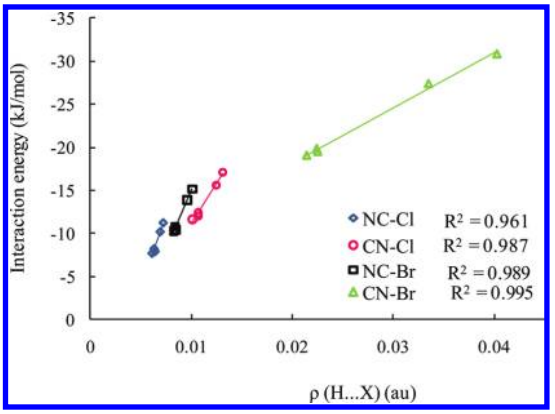

Figure 5. Relationship of interaction energy and electron density at the intermolecular BCP as well as linear correlation coefficients for each family of studied compounds calculated at MP2/6-311++G(d,p) level.

Table 4 shows that, for the investigated systems, $G(r_c)$ is near to and slightly greater than $|V(r_c)|$; thus $H(r_c)$ values are a little above zero. The two exceptions are CN−Br···H−Mg−H and CN−Br···H−Mg−CH_3 complexes, in which $H(r_c)$ is negative, indicating stronger interactions. Also, the calculated $G(r_c)/V(r_c)$ values in Table 4 are greater than unity except for the two mentioned exceptions. Moreover, there is a clear pattern of decrease in $G(r_c)/V(r_c)$ ratios for the stronger halogen−hydride interactions, which suggests an increasing covalent component of the interaction in such cases.

Apart from AIM, complementary information about the nature of halogen−hydride interaction can be derived from natural bond orbital (NBO) analysis. The data supplied in Table 5 present the calculated atomic charge of halogen and hydrogen as well as the amount of charge transfer (CT) from electron donor H−Mg−Y to halogen donor Z−X. It is evident that there is charge transfer in the range of 0.0051−0.0151 for NC−X complexes while it spans from 0.0070 to 0.1320 when the halogen is bound to nitrogen, as in CN−X complexes. In general, the stronger interaction in the complex, the more charge transfer from the electron donor to the halogen donor. The amount of charge transfer for Z−Br complexes is significantly greater than for Z−Cl complexes. The amount of charge transfer is less than 0.0077 in fluorine complexes while it ranges up to 0.1320 for bromine complexes. These allow us to conclude that charge transfer plays a more significant role when a better halogen donor such as CN−Br participates in the interaction, while it has a minor role in fluorine interactions.

Except for fluorine, the atomic charges of halogens are positive in both monomers and complexes, whereas that of hydrogen is negative. In general, the stronger interaction in the complex, the more positive the charge on the halogen atom. Upon complexation, both the positive charge on halogen and the negative charge on hydrogen increase. It should be mentioned that although the negative charge on the fluorine atom makes it less prone to involve in the interaction, the small positive electrostatic potential on the extension of Z−F bond causes a weakly bound interaction between Z−F and H−Mg−Y. This further confirms the idea that the Lewis acidity of Z−F is connected with the anisotropy of the electron charge distribution of fluorine.

3.5. Substituent Effect. Interested in improving our understanding of the relationship between the nature of the σ-hole at one terminal and the properties of the other substituent bonded to a common metal center, we compare the interaction strength of NC−X···H−Mg−Y and CN−X···H−Mg−Y complexes, where Y can be H, F, Cl, Br, or CH_3. Figure 6 presents the interaction energy variation for all studied complexes. We can draw a few key conclusions from the results in Figure 6. It is evident that the strength of all X···H bonds jump significantly when the halogen bonds to nitrogen, increasing ~1.8−2.0-fold for X = Br and by about 1.5- and 1.3-fold for X = Cl and F. When the free H atom in H−Mg−H is replaced by an electron-withdrawing substituent such as halogen, the binding distance is extended and the interaction energy is decreased. Thus, the interaction energies of H−Mg−F, H−Mg−Cl, and H−Mg−Br with both NC−X and CN−X are less negative than those obtained for the H−Mg−H system. However, the three halogens behave in a similar manner and the computed interaction energies lie in the same order. On the other hand, the substitution of methyl as the electron-donating group is more prominent, making a

Table 5. Natural Atomic Charges of Halogen and Hydrogen in Z−X···H−Mg−Y Complexes and Charge Transfer Occurring upon Formation of the Complexes[a]

complex	q_X	q_H	CT
NC−F···H−Mg−H	−0.2930	−0.7166	0.0054
NC−F···H−Mg−F	−0.2963	−0.7378	0.0059
NC−F···H−Mg−Cl	−0.2959	−0.7118	0.0056
NC−F···H−Mg−Br	−0.2955	−0.7069	0.0051
NC−F···H−Mg−CH_3	−0.2929	−0.7326	0.0060
NC−Cl···H−Mg−H	0.1495	−0.7378	0.0082
NC−Cl···H−Mg−F	0.1447	−0.7589	0.0075
NC−Cl···H−Mg−Cl	0.1454	−0.7341	0.0068
NC−Cl···H−Mg−Br	0.1459	−0.7294	0.0064
NC−Cl···H−Mg−CH_3	0.1504	−0.7522	0.0089
NC−Br···H−Mg−H	0.2383	−0.7470	0.0133
NC−Br···H−Mg−F	0.2315	−0.7733	0.0135
NC−Br···H−Mg−Cl	0.2346	−0.7440	0.0102
NC−Br···H−Mg−Br	0.2352	−0.7395	0.0097
NC−Br···H−Mg−CH_3	0.2388	−0.7598	0.0151
CN−F···H−Mg−H	−0.1218	−0.7140	0.0070
CN−F···H−Mg−F	−0.1256	−0.7352	0.0074
CN−F···H−Mg−Cl	−0.1252	−0.7091	0.0070
CN−F···H−Mg−Br	−0.1247	−0.7043	0.0065
CN−F···H−Mg−CH_3	−0.1217	−0.7297	0.0077
CN−Cl···H−Mg−H	0.3244	−0.7396	0.0209
CN−Cl···H−Mg−F	0.3116	−0.7639	0.0294
CN−Cl···H−Mg−Cl	0.3220	−0.7376	0.0156
CN−Cl···H−Mg−Br	0.3225	−0.7332	0.0151
CN−Cl···H−Mg−CH_3	0.3241	−0.7505	0.0236
CN−Br···H−Mg−H	0.3811	−0.7074	0.1003
CN−Br···H−Mg−F	0.3978	−0.7605	0.0555
CN−Br···H−Mg−Cl	0.4006	−0.7359	0.0539
CN−Br···H−Mg−Br	0.4012	−0.7311	0.0538
CN−Br···H−Mg−CH_3	0.3655	−0.6894	0.1320

[a] Calculated at MP2/6-311++G(d,p) level.

dx.doi.org/10.1021/jp200689b |J. Phys. Chem. A 2011, 115, 4457–4466

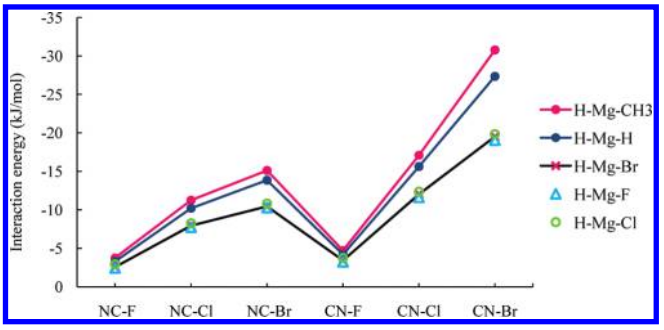

Figure 6. Interaction energy variation for different electron and halogen donors at MP2/6-311++G(d,p) level.

positive contribution and increasing the interaction energies. One can see that the effect of methyl group also depends on the nature of the halogen donor subunit. Here the enhancing effect of methyl group is larger for the CN−X halogen donor than for its NC−X counterpart. For the stronger interactions in CN−X···H−Mg−Y complexes, substitution of Y by methyl increases the interaction energies by about 2−3 kJ/mol toward H−Mg−H and 5−10 kJ/mol into H−Mg−X complexes.

4. CONCLUSIONS

A systematic investigation of electronic structure and molecular interactions of halogen in CN−X and NC−X halogen donors with H−Mg−Y has been presented. Different approaches were emplyed to study the nature and the strength of the resulting halogen−hydride bonds. They may be based on geometrical or AIM topological parameters, NBO analysis, shift in vibrational frequencies, and molecular electrostatic potentials. Interaction energies computed at the MP2 level vary from −1.23 to −2.99 kJ/mol for Z−F···H−Mg−Y complexes, indicating that the fluorine interactions are relatively very weak but not negligible. Instead, for chlorine- and bromine-containing complexes, the interaction energies span from −5.78 to a maximum of −26.42 kJ/mol, which intimates that the interactions are comparable to conventional hydrogen bonding. These values confirm that the halogen−hydride interactions in (NC)CN−X···H−Mg−Y complexes are much stronger than the recently reported interactions in YCCX···H−Mg−Y systems.[66]

Similar to hydrogen bonding, whose experimental signature is the red shifting of X−H stretching frequency of the hydrogen-bond donor, in the studied halogen−hydride interaction this signature is the red shifting of Z−X and the blue shifting of H−Mg bonds. However, the amounts of red shifts are greater and they are more systematic than the blue shifts. Moreover, investigating the substituent effect on the relative strength of the halogen−hydride bond energies, a negative cooperativity is found for halogen-substituted metal hydride while methyl substitution has a positive contribution and increases the interaction energy. There are also good linear correlations for the dependence of interaction energy on binding distance, frequency shift, molecular electrostatic potential, and intermolecular density at bond critical points.

■ ASSOCIATED CONTENT

Ⓢ Supporting Information. Two figures, showing relationships between interaction energies calculated withCCSD(T) at MP2 and B3LYP levels, and one table of Cartesian coordinates of optimized structures at MP2/6-31++G(d,p) level. This material is available free of charge via the Internet at http://pubs.acs.org.

■ AUTHOR INFORMATION

Corresponding Author

*Phone +98-711 6137520; fax +98-711 2286008; e-mail amohajeri@shirazu.ac.ir.

■ REFERENCES

(1) Buckingham, A. D.; Fowler, P. W.; Hutson, J. M. *Chem. Rev.* **1988**, *88*, 963.
(2) Chalasinski, G.; Szczesniak, M. M. *Chem. Rev.* **2000**, *100*, 4227.
(3) Wormer, P. E. S.; van der Avoird, A. *Chem. Rev.* **2000**, *100*, 4109.
(4) Philp, D.; Stoddart, J. F. *Angew. Chem., Int. Ed. Engl.* **1996**, *35*, 1155.
(5) Rudkevich, D. M. *Angew. Chem., Int. Ed.* **2004**, *43*, 558.
(6) Saalfrank, R. W.; Maid, H.; Scheurer, A. *Angew. Chem., Int. Ed.* **2008**, *47*, 8794.
(7) Llanes-Pallas, A.; Palma, C. A.; Piot, L.; Belbakra, A.; Listorti, A.; Prato, M.; Samori, P.; Armaroli, N.; Bonifazi, D. *J. Am. Chem. Soc.* **2009**, *131*, 509.
(8) Pimentel, G. C.; McClellan, A. L. *Hydrogen Bond*; W.H. Freeman: San Francisco, CA, 1960.
(9) Jeffrey, G. A. *An Introduction to Hydrogen Bonding*; W. H. Freeman: San Francisco, CA, 1960.
(10) Jeffrey, G. A. *Crystal Rev.* **2003**, *9*, 135.
(11) Grabowski, S. J. *Hydrogen Bonding: New Insights*; Springer: Amsterdam, 2006; Vol. 3.
(12) Alkorta, I.; Rozas, I.; Elguero, J. *Chem. Soc. Rev.* **1998**, *27*, 163.
(13) Zou, J. W.; Jiang, Y. J.; Guo, M.; Hu, G. X.; Zhang, B.; Liu, H. C.; Yu, Q. S. *Chem.—Eur. J.* **2005**, *11*, 740.
(14) Aakeroy, C. B.; Fasulo, M.; Schultheiss, N.; Desper, J.; Moore, C. *J. Am. Chem. Soc.* **2007**, *129*, 13772.
(15) Riley, K. E.; Hobza, P. *J. Chem. Theory Comput.* **2008**, *4*, 232.
(16) Alkorta, I.; Blanco, F.; Elguero, J. *Struct. Chem.* **2009**, *20*, 63.
(17) Bernal-Uruchurtu, M. I.; Hernandez-Lamoneda, R.; Janda, K. C. *J. Phys. Chem. A* **2009**, *113*, 5496.
(18) Metrangolo, P.; Meyer, F.; Pilati, T.; Resnati, G.; Terraneo, G. *Angew. Chem., Int. Ed.* **2008**, *47*, 6114.
(19) Metrangolo, P.; Resnati, G. *Chem.—Eur. J.* **2001**, *7*, 2511.
(20) Metrangolo, P.; Neukirch, H.; Pilati, T.; Resnati, G. *Acc. Chem. Res.* **2005**, *38*, 386.
(21) Zordan, F.; Brammer, L.; Sherwood, P. *J. Am. Chem. Soc.* **2005**, *127*, 5979.
(22) Rosokha, S. V.; Neretin, I. S.; Rosokaha, T. Y.; Hecht, J.; Kochi, K. *Heteroat. Chem.* **2006**, *17*, 449.
(23) Metrangolo, P.; Pilati, T.; Resnati, G. *Cryst. Eng. Commun.* **2006**, *8*, 946.
(24) Metrangolo, P.; Resnati, G.; Pilati, T.; Liantonio, R.; Meyer, F. *J. Polym. Sci., Part A: Polym. Chem.* **2007**, *45*, 1.
(25) Bilewicz, E.; Rybarczyk-Pirek, A. J.; Dubis, A. T.; Grabowski, S. J. *J. Mol. Chem. Struct.* **2007**, *829*, 208.
(26) Bertani, R.; Chaux, F.; Gleria, M.; Metrangolo, P.; Milani, R.; Pilati, T.; Resnati, G.; Sansotera, M.; Venzo, A. *Inorg. Chim. Acta* **2007**, *360*, 1191.
(27) Bruce, D. W. *Struct. Bonding (Berlin)* **2008**, *126*, 161.
(28) Metrangolo, P.; Resnati, G.; Pilati, T.; Biella, S. *Struct. Bonding (Berlin)* **2008**, *126*, 105.
(29) Metrangolo, P.; Neukirch, H.; Pilati, T.; Resnati, G. *Acc. Chem. Res.* **2005**, *38*, 386.
(30) Politzer, P.; Lane, P.; Concha, M. C.; Ma, Y.; Murray, J. S. *J. Mol. Model* **2007**, *13*, 305.
(31) Auffinger, P.; Hays, F. A.; Westhof, E.; Ho, P. S. *Proc. Natl. Acad. Sci. U.S.A.* **2004**, *101*, 16789.
(32) Murray, J. S.; Lane, P.; Politzer, P. *Int. J. Quantum Chem.* **2007**, *107*, 2286.

(33) Murray, J. S.; Lane, P.; Clark, T.; Politzer, P. *J. Mol. Model.* **2007**, *13*, 1033.
(34) Politzer, P.; Murray, J. S.; Concha, M. C. *J. Mol. Model.* **2008**, *14*, 659.
(35) Politzer, P.; Murray, J. S.; Lane, P. *Int. J. Quantum Chem.* **2007**, *107*, 3046.
(36) Politzer, P.; Murray, J. S.; Concha, M. C. *J. Mol. Model.* **2007**, *13*, 643.
(37) Politzer, P.; Murray, J. C.; Concha, M. C.; Lane, P.; Hobza, P. *J. Mol. Model.* **2008**, *14*, 699.
(38) Clark, T.; Hennemann, M.; Murray, J. S.; Politzer, P. *J. Mol. Model.* **2007**, *13*, 291.
(39) Awwadi, F. F.; Willett, R. D.; Peterson, K. A.; Twamley, B. *Chem.—Eur. J.* **2006**, *12*, 8952.
(40) Riley, K. E.; Merz, K. M. *J. Phys. Chem. A* **2007**, *111*, 1688.
(41) Glaser, R.; Chen, N. J.; Wu, H.; Knotts, N.; Kaupp, M. *J. Am. Chem. Soc.* **2004**, *126*, 4412.
(42) Lu, Y. X.; Zou, J. W.; Wang, Y. H.; Yu, Q. S. *J. Mol. Struct. (THEOCHEM)* **2006**, *776*, 83.
(43) Lu, Y. X.; Zou, J. W.; Wang, Y. H.; Yu, Q. S. *J. Mol. Struct. (THEOCHEM)* **2006**, *767*, 139.
(44) Poleshchuk, O. K.; Branchadell, V.; Brycki, B.; Fateev, A. V.; Legon, A. C. *J. Mol. Struct. (THEOCHEM)* **2006**, *760*, 175.
(45) Mohajeri, A.; Pakiari, A. H.; Bagheri, N. *Chem. Phys. Lett.* **2009**, *467*, 393.
(46) Romaniello, P.; Lelj, F. *J. Phys. Chem. A* **2002**, *106*, 9114.
(47) Wang, W. Z.; Tian, A. M.; Wong, N. B. *J. Phys. Chem. A* **2005**, *109*, 8035.
(48) Riley, K. E.; Hobza, P. *J. Chem. Theory Comput.* **2008**, *4*, 232.
(49) Wang, Y. H.; Lu, Y. X.; Zou, J. W.; Yu, Q. S. *Int. J. Quantum Chem.* **2008**, *108*, 1083.
(50) Donald, K. J.; Wittmaack, B. K.; Crigger, C. *J. Phys. Chem. A* **2010**, *110*, 7213.
(51) Lucassen, A. C. B.; Karton, A.; Leitus, G.; Shimon, L. J. W.; Martin, J. M. L.; van der Boom, M. E. *Cryst. Growth Des.* **2007**, *7*, 386.
(52) Lucassen, A. C. B.; Vartanian, M.; Leitus, G.; van der Boom, M. E. *Cryst. Growth Des.* **2005**, *5*, 1671.
(53) Mossakowska, I.; Wojcik, G. *Acta Crystallogr., Sect. C: Cryst. Struct. Commun.* **2007**, *63*, O123.
(54) Mugnaini, V.; Punta, C.; Liantonio, R.; Metrangolo, P.; Recupero, F.; Resnati, G.; Pedulli, G. F.; Lucarini, M. *Tetrahedron Lett.* **2006**, *47*, 3265.
(55) Russo, L.; Biella, S.; Lahtinen, M.; Liantonio, R.; Metrangolo, P.; Resnati, G.; Rissanen, K. *Cryst. Eng. Commun.* **2007**, *9*, 341.
(56) Borowiak, T.; Wolska, I.; Brycki, B.; Zielinski, A.; Kowalczyk, I. *J. Mol. Struct.* **2007**, *833*, 197.
(57) Li, R. Y.; Li, Z. R.; Wu, Y.; Li, Y.; Chen, W.; Sun, C. C. *J. Phys. Chem. A* **2005**, *109*, 2608.
(58) Wang, Y. H.; Zou, J. W.; Lu, Y. X.; Lu, Q. S.; Xu, H. Y. *Int. J. Quantum Chem.* **2007**, *107*, 501.
(59) Li, Q. Z.; Wang, Y. L.; Liu, Z. B.; Li, W. Z.; Cheng, J. B.; Gong, B. A.; Sun, J. Z. *Chem. Phys. Lett.* **2009**, *469*, 48.
(60) Richardson, T. B.; deGala, S.; Crabtree, R. H.; Siegbahn, P. E. M. *J. Am. Chem. Soc.* **1995**, *117*, 12875.
(61) Wu, Y.; Feng, L.; Zhang, X. D. *J. Mol. Struct. (THEOCHEM)* **2008**, *851*, 294.
(62) Pakiari, A. H.; Mohajeri, A. *J. Mol. Struct. (THEOCHEM)* **2003**, *620*, 31.
(63) Alkorta, I.; Zborowski, K.; Elguero, J.; Solimannejad, M. *J. Phys. Chem. A* **2006**, *110*, 10279.
(64) Rozas, I.; Alkorta, I.; Elguero, J. *J. Phys. Chem. A* **1997**, *101*, 4236.
(65) Lipkowski, P.; Grabowski, S. J.; Leszczynski, J. *J. Phys. Chem. A* **2006**, *110*, 10296.
(66) Li, Q. Z.; Dong, X.; Jing, B.; Li, W. Z.; Cheng, J. B.; Gong, B. A.; Yu, Z. W. *J. Comput. Chem.* **2010**, *31*, 1662.
(67) Li, Q. Z.; Yuan, H.; Jing, B.; Liu, Z.; Li, W. Z.; Cheng, J. B.; Gong, B. A.; Sun, J. Z. *Mol. Phys.* **2010**, *108*, 611.
(68) Li, Q.; Yuan, H.; Jing, B.; Liu, Z.; Li, W.; Cheng, J.; Gong, B.; Sun, J. *J. Mol. Struct. (THEOCHEM)* **2010**, *942*, 145.
(69) Lu, J.; Lu, Y.; Zhu, W. *J. Mol. Struct. (THEOCHEM)* **2010**, *952*, 84.
(70) Solimannejad, M.; Malekani, M.; Alkorta, I. *J. Phys. Chem. A* **2010**, *114*, 12106.
(71) Wang, S. *J. Mol. Struct. (THEOCHEM)* **2010**, *952*, 115.
(72) Frisch, M. J.; Trucks, G. W.; Schlegel, H. B.; Scuseria, G. E.; Robb, M. A.; Cheeseman, J. R.; Montgomery, J. A., Jr.; Vreven, T.; Kudin, K. N.; Burant, J. C.; Millam, J. M.; Iyengar, S. S.; Tomasi, J.; Barone, V.; Mennucci, B.; Cossi, M.; Scalmani, G.; Rega, N.; Petersson, G. A.; Nakatsuji, H.; Hada, M.; Ehara, M.; Toyota, K.; Fukuda, R.; Hasegawa, J.; Ishida, M.; Nakajima, T.; Honda, Y.; Kitao, O.; Nakai, H.; Klene, M.; Li, X.; Knox, J. E.; Hratchian, H. P.; Cross, J. B.; Adamo, C.; Jaramillo, J.; Gomperts, R.; Stratmann, R. E.; Yazyev, O.; Austin, A. J.; Cammi, R.; Pomelli, C.; Ochterski, J. W.; Ayala, P. Y.; Morokuma, K.; Voth, G. A.; Salvador, P.; Dannenberg, J. J.; Zakrzewski, V. G.; Dapprich, S.; Daniels, A. D.; Strain, M. C.; Farkas, O.; Malick, D. K.; Rabuck, A. D.; Raghavachari, K.; Foresman, J. B.; Ortiz, J. V.; Cui, Q.; Baboul, A. G.; Clifford, S.; Cioslowski, J.; Stefanov, B. B.; Liu, G.; Liashenko, A.; Piskorz, P.; Komaromi, I.; Martin, R. L.; Fox, D. J.; Keith, T.; Al-Laham, M. A.; Peng, C. Y.; Nanayakkara, A.; Challacombe, M.; Gill, P. M. W.; Johnson, B.; Chen, W.; Wong, M. W.; Gonzalez, C.; Pople, J. A. *Gaussian 03*, revision B.03; Gaussian, Inc.: Pittsburgh, PA, 2003.
(73) Møller, C.; Plesset, M. S. *Phys. Rev.* **1934**, *46*, 618.
(74) Riley, K. E.; Pitonak, M.; J.; Cerny, J.; Hobza, P. *J. Chem. Theory Comput.* **2010**, *6*, 66.
(75) Becke, A. D. *J. Chem. Phys.* **1993**, *98*, 5648.
(76) Lee, C.; Yang, W.; Parr, R. G. *Phys. Rev. B: Condens. Matter Mater. Phys.* **1998**, *37*, 785.
(77) Boys, S. F.; Bernardi, F. *Mol. Phys.* **1970**, *19*, 553.
(78) Bader, R. F. W. *Atoms in Molecules, A Quantum Theory*; Oxford University Press: New York, 1990.
(79) Bader, R. F. W. AIM2000 Program, v 2.0; McMaster University, Hamilton, Canada, 2000.
(80) Reed, A. E.; Curtiss, L. A.; Weinhold, F. A. *Chem. Rev.* **1998**, *88*, 899.
(81) Politzer, P., Truhlar, D. G., Eds. *Chemical Applications of Atomic and Molecular Electrostatic Potentials*; Plenum Press: New York, 1981.
(82) Bondi, A. *J. Phys. Chem.* **1964**, *68*, 441.
(83) Alkorta, I.; Solimannejad, M.; Provasi, P.; Elguero, J. *J. Phys. Chem. A* **2007**, *111*, 7154.
(84) Wang, Y. H.; Lu, Y. X.; Zou, J. W.; Yu, Q. S. *Int. J. Quantum Chem.* **2008**, *108*, 1083.
(85) Stewart, R. F. *Chem. Phys. Lett.* **1979**, *65*, 335.
(86) Gross, K. C.; Seybold, P. G.; Peralta-Inga, Z.; Murray, J. S.; Politzer, P. *J. Org. Chem.* **2001**, *66*, 6919.
(87) Ma, Y.; Gross, K. C.; Hollingsworth, C. A.; Seybold, P. G.; Murray, J. S. *J. Mol. Model.* **2004**, *10*, 235.
(88) Liu, S.; Pedersen, L. G. *J. Phys. Chem. A* **2009**, *113*, 3648.
(89) Mohajeri, A.; Alipour, M. *Struct. Chem.* **2010**, *21*, 727.
(90) Alipour, M.; Mohajeri, A. *J. Phys. Chem. A* **2010**, *114*, 7417.
(91) Scrocco, E; Tomasi, J. *J. Adv. Quantum Chem.* **1978**, *11*, 116.
(92) Naray-Szabó, G.; Ferenczy, G. G. *Chem. Rev.* **1995**, *95*, 829.
(93) Politzer, P.; Murray, J. S.; Concha, M. C. *Int. J. Quantum Chem.* **2002**, *88*, 19.
(94) Murray, J. S.; Lane, P.; Politzer, P. *J. Mol. Model.* **2009**, *15*, 723.
(95) Murray, J. S.; Politzer, P. *J. Mol. Struct.* **1998**, *425*, 107.
(96) Murray, J. S.; Politzer, P. *Croat. Chem. Acta* **2009**, *82*, 267.
(97) Koch, U.; Popelir, P. L. A. *J. Phys. Chem. A* **1995**, *99*, 9747.
(98) Mohajeri, A.; Fadaei, F. *J. Phys. Chem. A* **2008**, *112*, 281.
(99) Cremer, D.; Kraka, E. *Angew. Chem.* **1984**, *23*, 627.
(100) (a) Nakanishi, W.; Nakamoto, T.; Hayashi, S.; Sasamori, T.; Tokitoh, N. *Chem.—Eur. J.* **2007**, *13*, 255. (b) Nakanishi, W.; Hayashi, S.; Nahara, K. *J. Phys. Chem. A* **2009**, *113*, 10050. (c) Nakanishi, W.; Hayashi, S. *Curr. Org. Chem.* **2010**, *14*, 181.